J. Membrane Biol. 162, 157–167 (1998)

The Journal of
Membrane
Biology

Membrane Potential Mediates H^+-ATPase Dependence of ''Degradative Pathway'' Endosomal Fusion

T.G. Hammond[1], F.O. Goda[1], G.L. Navar[1], W.C. Campbell[1], R.R. Majewski[2], D.L. Galvan[3], F. Pontillon[4], J.H. Kaysen[1], T.J. Goodwin[5], S.W. Paddock[6], P.J. Verroust[4]

[1]Tulane University School of Medicine, Tulane Environmental Astrobiology Center and New Orleans Veteran's Affairs Medical Center, 1430 Tulane Avenue, New Orleans, Louisiana 70112, USA
[2]Department of Medicine, University of Wisconsin, Madison, Wisconsin, USA
[3]Laboratory of Cell Biology, Sinai-Samaritan Medical Center, University of Wisconsin Milwaukee Clinical Campus, Milwaukee, Wisconsin, USA
[4]Institut National de la Santé et de la Recherché Médicale U64, Hôpital Tenon, Paris, France
[5]NASA Johnson Space Center, Houston, Texas, USA
[6]Department of Molecular Biology, and Howard Hughes Medical Institute, University of Wisconsin, Madison, Wisconsin, USA

Received: 29 October 1996/Revised: 8 December 1997

Abstract. In some epithelial cell lines, the uptake and degradation of proteins is so pronounced as to be regarded as a specialized function known as ''degradative endocytosis.'' The endosomal pathways of the renal proximal tubule and the visceral yolk sac share highly specialized structures for ''degradative endocytosis.'' These endosomal pathways also have a unique distribution of their H^+-ATPase, predominantly in the subapical endosomal pathway. Previous studies provide only indirect evidence that H^+-ATPases participate in endosomal fusion events: formation of vesicular intermediates between early and late endosomes is H^+-ATPase dependent in baby hamster kidney cells, and H^+-ATPase subunits bind fusion complex proteins in detergent extracts of fresh rat brain. To determine directly whether homotypic endosomal fusion is H^+-ATPase dependent, we inhibited v-type H^+-ATPase during flow cytometry and cuvette-based fusion assays reconstituting endosomal fusion in vitro. We report that homotypic fusion in subapical endosomes derived from rat renal cortex, and immortalized visceral yolk sac cells in culture, is inhibited by the v-type H^+-ATPase specific inhibitor bafilomycin A1. Inhibition of fusion by H^+-ATPase is mediated by the membrane potential as collapsing the pH gradient with nigericin had no effect on homotypic endosomal fusion, while collapsing the membrane potential with valinomycin inhibited endosomal fusion. Utilizing an in vitro reconstitution assay this data provides the first direct evidence for a role of v-type H^+-ATPase in mammalian homotypic endosomal fusion.

Key words: Kidney — Flow cytometry — Endosomal trafficking — Yolk sac — Energy transfer

Introduction

The cascade of intracellular membrane fusion involves a series of biochemical reactions resulting in the opening and contiguous reattachment of intracellular membranes [1, 6, 33]. The cytosolic ATPase proteins NEM-sensitive factor [NSF], and SNAP, as well as the highly conserved cognate membrane-bound syntaxin and synaptobrevin families of proteins, all are critical to the final steps of fusion [1, 6, 33]. Membrane thermodynamics, largely determined by fusion proteins, is postulated to be a major determinate, not only of cellular compartmentation, but also of polarity, tissue differentiation and membrane trafficking [8, 33]. Several lines of evidence link v-type H^+-ATPases to control of both exocytotic and endosomal trafficking events indirectly. In the exocytotic pathway v-type ATPase inhibitors block surface expression of viral envelope glycoproteins in Baby Hamster Kidney [BHK] cells [3], and cause precursor proteins to accumulate in prevacuolar compartments of yeast [40]. In the endosomal pathway of human hepatoma cells, v-type ATPase inhibition slows trafficking through early and late endosomes, and abolishes receptor-ligand uncoupling and lysosomal trafficking [39].

Correspondence to: T.G. Hammond

Further, in NRK, COS and CHO cells, sorting processes mediated by signals in the cytoplasmic portion of proteins are dependent on the internal pH of endosomes [3]. In BHK cells, H^+-ATPase inhibition is associated with marked tubule formation in the early endosomal compartment, and endocytosed markers do not enter the late endosomal compartment [4]. This suggests that the formation of vesicular intermediates between early and late endosomes is H^+-ATPase dependent [4]. Hence, H^+-ATPases play an important role in membrane trafficking in diverse exocytotic and endosomal compartment from yeast to mammalian cells.

Recent evidence from co-immunoprecipitation and binding studies suggests a more direct role for H^+-ATPases in membrane fusion events. During immunoprecipitation of synaptobrevin and synaptophysin from detergent extracts of fresh rat brain, three subunits of the H^+-ATPase coimmunoprecipitated with the fusion complex proteins, suggesting physical association [8]. Despite these suggestive observations, direct evidence linking v-type H^+-ATPases functionally to specific fusion events is lacking. Early attempts to define a direct role for H^+-ATPase in endosomal fusion were reported amongst surveys of biochemical mediators of fusion [6]. These reports were on tiny numbers of observations ($n = 3$) with no measures of variability stated, and now deserve more vigorous reexamination.

To provide direct evidence for a functional role of H^+-ATPase, we isolated endosomes from rat renal cortex and yolk sac epithelial cells and studied fusion reconstituted in vitro using an original assay based on fluorescent energy transfer. These tissues were selected because v-type H^+-ATPase activity is particularly abundant [2, 10, 34]. The subapical endosomal pathways in these epithelia is characterized by a high level of endocytosis followed by degradation of the internalized material, a process referred to as ''degradative endocytosis'' [12, 21, 22]. This property is associated with a high turnover of plasma membrane which entails efficient recycling carried out by specialized structures, known as dense apical tubules, and a high level of lysosomal delivery. Furthermore, common clinical toxins, such as aminoglycoside antibiotics and myeloma light chains, only damage tissues with this endosomal pathway specialized for degradative endocytosis [10, 21, 22, 26, 35]. In this study, we provide direct evidence linking v-type H^+-ATPase to fusion of endosomes in ''degradative'' endosomal pathways.

The specialized features of the 'degradative' endosomal pathway and the proteins, such as gp280, the polybasic drug receptor megalin, and abundant H^+-ATPase, which are associated with these features, can only be found in two tissues. First, native rat kidney has the full compliment of specialized features [2, 24]. As a differentiated tissue, native rat kidney also has the advantage that different membranes retain diverse buoyant densities, and hence endosomes can be isolated by differential centrifugation [11, 12, 17]. Unfortunately, there is no propagated renal cell line which maintains these features [21, 30]. Popular renally derived cell lines such as MDCK, LLP-CK1, immortalized human proximal cell lines, and countless others lose the 'degradative' pathway features in culture. Hence, the first model utilized in our studies is endosomes isolated from native rat renal cortex.

The second model to be studied, yolk sac epithelial cells, provides an immortal cell line which retains the specialized features of the ''degradative'' endosomal pathway in culture [21, 22, 30]. This allows us to investigate the H^+-ATPase dependence of fusion in a second cell type with specialized features. As yolk sac epithelial cell membranes all have virtually identical buoyant density in culture [23, 30], we must rely on the compartmentation of dye to report fusion and study endosomal fusion mechanisms [1, 6, 13, 19, 25, 32]. Grown under specialized culture conditions [15] immortalized yolk sac epithelial cells forms small embryoid bodies with an outwardly directed brush border, with a sphere of cells around a fluid filled cavity providing unequivocal polarity. Hence, fluorescent dyes can be delivered apically into the early endosomal pathway for subsequent investigation of the role of H^+-ATPase activity in endosomal fusion.

Materials and Methods

Animals, Reagents and Antibodies

Male Sprague Dawley rats (200–250 gm) [Sasco, Omaha, NE] were anesthetized with pentobarbital on the day of the experiment. All reagents were from Sigma Chemical (St. Louis, MO) unless otherwise stated. All fluorescence measurements were made in the presence of 7μl/3ml anti-fluorescein antibodies (a gift of Dr. H. William Harris, the Children's Hospital, Boston, MA) to quench extravesicular fluorescein fluorescence [10–14].

Preparation of Rat Renal Cortical Endosomes

Rat kidneys were loaded with fluorescein and rhodamine dextran by intravenous infusion into the rats, and renal cortex harvested 15 min later [12]. Renal cortical ''light'' endosomes were prepared by differential Percoll gradient centrifugation as previously described [12]. In brief, this endosomal fraction, which is slightly lighter than basolateral membranes, is characterized by homogeneity for entrapped markers and the presence of H^+-ATPase [12]. Colocalization on a particle-by-particle basis of modest amounts of apically derived enzymes (g-glutamyl transpeptidase, leucine aminopeptidase, and dipeptidase peptidase IV) and giant glycoprotein receptors (gp280 and megalin) with entrapped markers suggests that this population represents an apically derived endosomal compartment [12], consisting of a mixture of endosomal vesicles and endosomal vacuoles [2, 22, 24, 30].

Culture of Rat Visceral Yolk Sac Cells

The yolk sac epithelial cell line (BN/MSV) was derived from yolk sac teratocarcinoma induced by fetectomy and yolk sac infection with Mouse Sarcoma Virus [21]. When grown under conventional conditions in modified Eagles Medium supplemented with 2.5 mM L-glutamine, 10% fetal calf serum, and an antibiotic cocktail [penicillin streptomycin and fungizone], the cells initially form a monolayer and at confluence release into the supernatant a few cellular aggregates, often surrounding a fluid filled central cavity, referred to as embryoid bodies [15]. The number of embryoid bodies is increased when the cells are grown under non-adherent culture conditions [15].

Pilot experiments showed that rotating wall vessel bioreactors (Synthecon, Houston, TX), a form of non-adherent culture, previously shown to increase epithelial cell differentiation [9], substantially induced embryoid body formation in BN/MSV cell culture. This technique was therefore used to grow BN/MSV cells in the present study [9]. To initiate BN/MSV cell rotating wall vessel culture the vessel was filled with medium, and seeded by addition of cell suspension (2×10^6 cells/ml). Residual air was removed through a syringe port and vessel rotation was initiated at 10 rotations per min, and maintained for 48 hr in the same medium prior to use.

Preparation of Endosomes from BN Cells

Aliquots of BN/MSV cells cultured in rotating wall vessels were incubated in fluorescein or rhodamine dextran at optimal concentrations for fluorescent energy transfer, as previously described [13, 17]. In brief, the cells were placed in serum-free medium containing the fluorescent dye for 10 min in a 37°C incubator. Cells were cooled on ice, and homogenized with 10 passes of a glass-Teflon homogenizer. A post nuclear supernatant was prepared. Unlike the renal cortex in which a highly purified endosomal preparation was isolated, assay of fusion in BN/MSV cell endosomes depends on endosomal compartmentation of fluorescent dye used as a reporter in the post nuclear supernatant.

In vitro Reconstitution of Endosomal Fusion

To study in vitro the fusion of true subapical endosomal membranes we used the method previously validated for studying the NEM-sensitive, ATP- and cytosol-dependent fusion of vesicles derived from intermicrovillar clefts [''heavy endosomes''] [14]. This assay is based on the ''spectroscopic ruler'' effects of energy transfer between two different fluorescent dextrans: if energy transfer is observed the donor and acceptor molecules are unequivocally within 1–6 nm i.e., in the same membrane-bound compartment, since energy transfer will not occur across a 7.5 nm lipid bilayer membrane. In practice the assay involves analysis of a mixture of aliquots of two separate populations of endosomes loaded with either green (fluorescein labeled) or red (rhodamine labeled) dextrans in which fusion has been inhibited by N-ethylmaleimide (NEM). Under these conditions, the blue laser light excites fluorescent emission from the green but not the red dextran. Addition of cytosol provides fresh NEM-sensitive factor, and restores fusion competence of the membranes so that the red dextran can now be excited by the emission from the green dextran, provided they are within 1–6 nm of each other. Fluorescent signals are assayed from whole populations in a cuvette, or on a vesicle-by-vesicle basis by flow cytometry [13, 17]. Preliminary experiments were performed to determine the optimal cytosol and ATP concentrations for each membrane type. Repeat measures on duplicate samples, to determine reproducibility of the fluorometry fusion assay, had a Pearson correlation coefficient of 0.96 for $n = 21$ independent tests. Aliquots of endosomes were pretreated by incubation in 10 μM valinomycin, 10 μM nigericin, or 30 nM bafilomycin A1 as indicated, for at least 30 min on ice.

Cytosol Preparation

Cytosol was prepared by homogenizing rat renal cortex in a modified fusion buffer containing, 100 mM KCl, 85 mM sucrose, 1.5 mM $MgCl_2$, and 20 μM EGTA, pH 7.4 with Tris, supplemented with 370 μM ATP and 2 mM dithiothreitol to stabilize NSF [1]. The tissue was first supplemented with 370 μM ATP and 2 mM dithiothreitol to stabilize NSF [1]. The tissue was first coarsely ground in a Waring blender and then further homogenized with a glass-Teflon tissue grinder. The homogenate was spun at 100,000 × *g* for 1 hr at 4°C. The supernatant was frozen in aliquots at −70°C, and thawed on ice immediately prior to use as cytosol [13].

Single-Beam Flow Cytometric Analysis of Fusion by Energy Transfer on a Vesicle-by-Vesicle Basis

Flow cytometry analysis was performed on a Beckton-Dickinson FASCtar Plus flow cytometer [10–14, 17]. Excitation was at 488 nm (200 mW) using a Coherent 6W Argon-ion laser. For each particle, emission was measured using photomultipliers with 530 ± 30 nm band pass and 577–677 nm band pass filters for fluorescein and rhodamine respectively. Data were collected as 2,000 event list mode files and analyzed using LYSYS II [Beckton-Dickinson, Mountain View, CA] and Multitime [Phoenix Flow Systems, San Diego, CA] software. Optical and electronic settings were optimized for small particle resolution [11, 29].

Confocal Microscopy

Aliquots of samples were analyzed using a BioRad MRC 600 laser scanning confocal microscope [31]. Fluorescein and rhodamine were excited independently with 488 nm and 568 nm laser lines from a 15 mW Argon-Krypton mixed gas laser (Ion Laser Tech, Salt Lake City, Utah) and the images were overlaid electronically using previously published methods [31].

Electron Microscopy

Samples were prepared for transmission electron microscopy as previously detailed [11–15, 17]. In brief, the samples were fixed with 2.0% paraformaldehyde and 0.2% glutaraldehyde in overnight, dehydrated an acetone and embedded in Epon. Lead-stained thin sections were examined and photographed using a Phillips EM/200 electron microscope.

Membrane Potential

The membrane potential dye 5,5′,6,6′-tetrachloro-1,1′,3,3′-tetraethylbenzimidazolylcarbocyanine iodide known as JC-1 (Molecular Probes, Eugene, OR) [5, 7, 27] was utilized to investigate the presence of a membrane potential during our endosomal fusion experiments. Rat renal endosomes were prepared loaded with 100 mM KCl [12]. A 10 μl aliquot of 1 mg/ml protein concentration of these membranes was dropped into 10 μM JC-1, with potassium content varied in linear steps from 0 to 100 mM KCl. Using excitation at the optimal 488 nm wavelength emission was scanned from 500 to 750 nm using a Fluo-

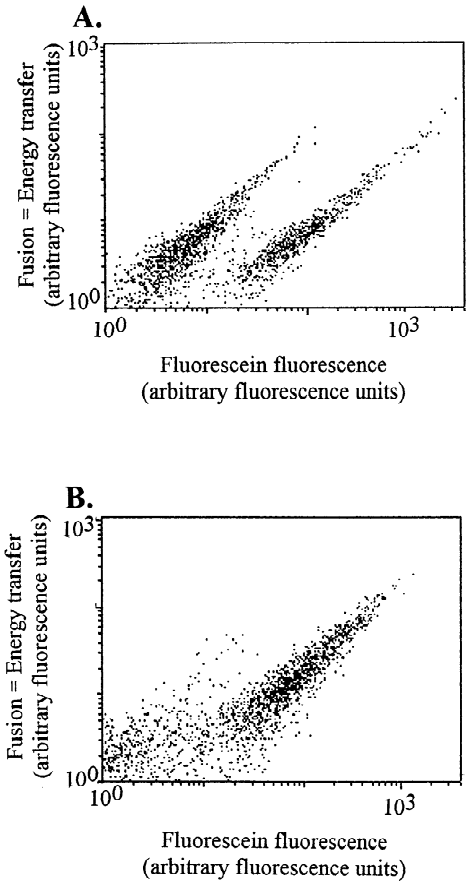

Fig. 1. Flow cytometry energy transfer assay of renal cortical light endosome fusion on a vesicle-by-vesicle basis. (*A*) NEM-inhibited control shows two populations of endosomes, one representing rhodamine containing endosomes (on left), and one representing fluorescein containing endosomes (on right). (*B*) Following fusion virtually all particles show both colored emissions, fluorescein by direct excitation, and rhodamine by energy transfer. Each panel depicts 2,000 endosomes. Representative of $n = 8$.

roMax-2 spectrofluorometer (Instruments S.A., Edison, NJ). This blue dye with a delocalized positive charge redistributes from the buffer onto the membranes upon membrane hyper polarization. The membrane associated dye is quenched due to dimerization, with a linear response from −40 to +50 mV. A standard curve of potassium gradients was replicated with and without 10 μM of the artificial potassium transporter valinomycin, which generates a membrane potential [5, 7, 27, 36].

Statistics

Data is expressed as means ± SE of the mean throughout the manuscript. Statistical analysis was performed by analysis of variance and Bonferroni post hoc comparison. When large flow cytometry data sets of 2,000 or more events were collected, statistical comparisons were made both by Kolgomorov-Smirnoff summation curves and comparison of means of flow cytometry distributions [41].

Results

Fusion of Renal Cortical Endosomes: Flow Cytometry

Single-beam flow cytometry analysis of fusion occurring between endosomes prepared from rat renal cortex with entrapped fluorescein- or rhodamine-dextran is shown in Fig. 1. First, we examined the distribution of fluorescein and rhodamine fluorescence in an unfused control sample consisting of an equal mixture of fluorescein-containing and rhodamine containing endosomes. The data is displayed as dot plot depicting 2000 individual values on a log Cartesian grid [Fig. 1*A* and *B*]. The NEM inhibited controls show two distinct populations differing in fluorescein content but uniformly dim for rhodamine fluorescence [Fig. 1*A*]. Following fusion energy transfer rhodamine fluorescence increases in virtually all the endosomes, and more than 95% of the endosomes are now positive for fluorescein fluorescence [Fig. 1*B*]. Fusion was quantified using the classic approach for large data sets by which Kolgomorov-Smirnoff summation curves showed significant fusion in each of four trials ($n = 4$, $P < 0.01$). The study was repeated using energy transfer on the whole population of endosomes in a cuvette. The mean of each energy transfer rhodamine dextran fluorescence distribution was quantitated and comparisons made on groups of means (control NEM inhibited samples 0 ± 8 arbitrary fluorescence units compared to 74 ± 8 in the fused samples, $n = 6$, $P < 0.01$). A half log shift in fluorescence of 577–677 nm fluorescence of rhodamine dextran on the ordinate in Fig. 1*B* demonstrates that fusion is occurring, and not just endosomal aggregation. The blue 488 nm laser light excites green fluorescein-dextran entrapped in half the endosomes, but not the red rhodamine-dextran entrapped in the other half of the endosomes. The red rhodamine-dextran can only be excited by the emission from the excited green fluorescein-dextran. This energy transfer is used as a ''spectroscopic ruler'' as it only occurs if the two dye molecules are within 1–6 nm of each other. As this energy transfer needs the two dyes to be less than the width of a single membrane apart, the endosomes have fused with the dyes unequivocally in the same compartment when energy transfer occurs [10, 13, 17, 38]. The more than half log shift in energy transfer on the ordinate demonstrates endosomal fusion is occurring not just aggregation.

Ultrastructure

Electron micrographs of rat renal cortical light endosomes before and after fusion confirm that the changes in fluorescence signatures are indicative of endosomal fusion. Prior to fusion the endosomes are relatively small

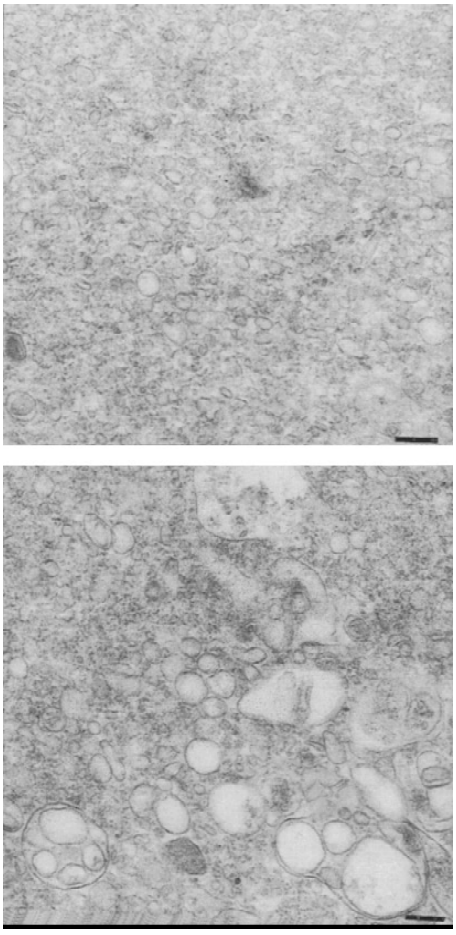

Fig. 2. Electron microscopy of fusion events. Electron microscopy provides structural confirmation of the fusion suggested by fluorescent signatures. Images of the negative control, unfused, population [left panel] demonstrates fairly uniform endosomal size without demonstrable contamination with mitochondria or other organelles [X11,000]. Bar 1.0 μM. Following fusion, the average diameter of the endosomes increases more than 5 fold [right panel] consistent with multiple fusion events [X 11,000]. Representative of more than 100 fields in 2 separate samples. Bar 1.0 μM.

immersed in a background of polymerized microtubules and other elements in the cytosol (Fig. 2, left panel). Following fusion the average vesicle size increases more than 5-fold [ratio of diameters 1.0 to 5.1 ± 1.6, $n = 100$ randomly selected vesicles from 5 grids] (Fig. 2, right panel).

H+-ATPase Dependence of Fusion

Rat renal cortical endosomal fusion display a highly distinctive pattern of H+-ATPase dependence (Fig. 3). The specific v-type H+-ATPase inhibitor bafilomycin A1 inhibited endosomal fusion by 82 ± 4% (18 ± 4% of control) compared to control, [$n = 4$, $P < 0.05$] suggesting that fusion of these membranes requires H+-ATPase activity. In contrast, collapsing the pH gradient with nigericin in the presence of potassium had no effect on fusion, demonstrating that a pH gradient is not necessary for fusion [96 ± 4% of control, $n = 4$, $P > 0.05$]. Collapsing the H+-ATPase dependent membrane potential in endosomes with valinomycin inhibits fusion by 71 ± 4% (to 29 ± 4%) compared to control, $n = 6$, $P < 0.05$.

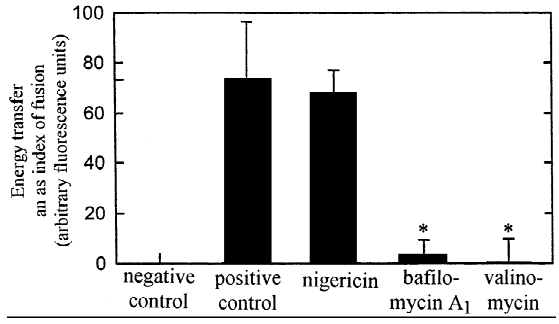

Fig. 3. H+-ATPase dependence of homotypic rat renal endosome fusion during in vitro reconstitution. Effects of H+-ATPase agents on cuvette based assay on fusion of rat renal proximal tubular endosomes using energy transfer from fluorescein to rhodamine to detect fusion. Although the specific H+-ATPase inhibitor, bafilomycin A1, and collapsing the membrane potential with valinomycin inhibit fusion, collapsing the pH gradient with nigericin has no effect on fusion. Mean ± SE for $n = 6$, *denotes $P < 0.05$ by ANOVA and Scheffe posthoc analysis.

Membrane Potentials Resultant from Valinomycin and a Potassium Gradient

To determine if renal endosomes have a membrane potential which is collapsed by valinomycin under the fusion conditions employed, studies were performed with the membrane potential reporter dye JC-1 [5, 7, 27]. Initially to confirm the linear relationship between membrane potential and dye fluorescence predicted by the Nernst equation [5, 7, 27] and published dye signatures [5, 7, 27], equal aliquots of endosomes loaded with 100 mM KCl were dropped into for fusion experiments including the presence of 10 μM valinomycin. Linear regression is significant for Pearson correlation coefficient $= 0.85$, $t = 7.60$, with 22 degrees of freedom and $P <$ 1.37E-007 [Fig. 4 upper panel].

Using this scale membrane potential was assayed in the endosomes under fusion conditions with and without valinomycin. Assay of samples in a cuvette by spectrofluorometry show that there is a membrane potential on the membrane under fusion conditions (Fig. 4, middle panel, left bar) which is collapsed in the presence of valinomycin [38 ± 7 compared to 0 ± 8 arbitrary fluorescent units, $n = 6$, $P < 0.05$].

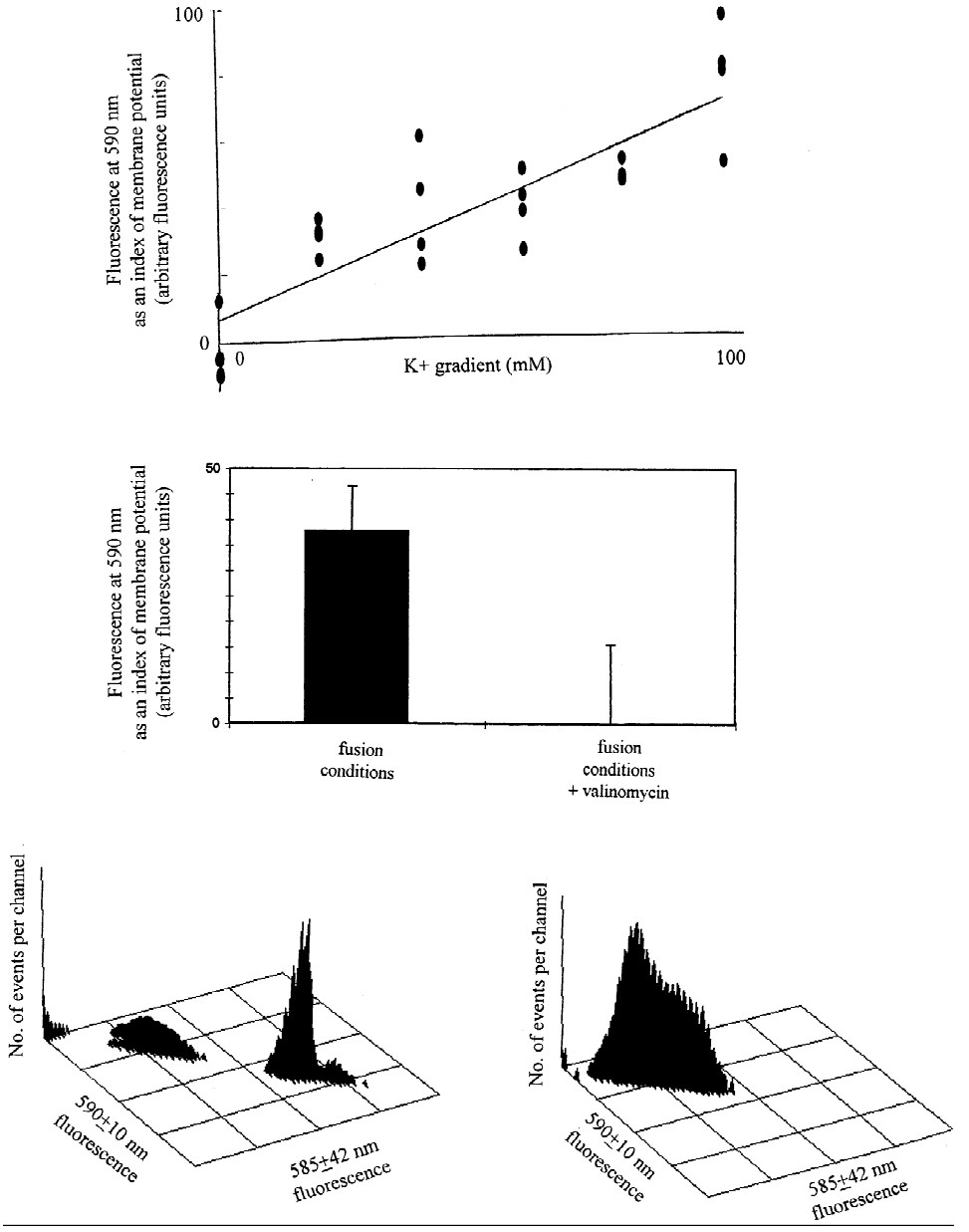

Fig. 4. Membrane potential in rat renal endosomes prepared for fusion studies. To determine if renal endosomes had a membrane potential collapsible by valinomycin a series of studies were performed. *Upper panel.* First, equal aliquots of endosomes loaded with 100 mM KCl were dropped into buffer with stepwise concentrations of 0 to 100 mM KCl and the spectrum of the reporter fluorophore JC-1 scanned. A plot of fluorescence of the membrane potential probe JC-1 against potassium gradient demonstrates linearity of response at 590 nm *Middle panel.* To Determine if there is a membrane potential on rat renal cortical endosomes under the fusion conditions including cytosol membrane potential was assayed using JC-1 with and without valinomycin. There is substantial membrane potential across the endosomal membranes [left bar] which is collapsed by valinomycin [right bar]. *Lower panel.* Flow cytometry of the membrane potential on an endosome-by-endosome basis demonstrates the number of endosomes in the fraction in which membrane potential was collapsed. Horizontal axes depict fluorescence of membrane sensitive probe at peak 590 ± 10 nm (abscicca) and total 585 ± 42 nm (ordinate) with number of endosomes per channel on the vertical axis up out of the page, frequency histogram for 2000 endosomes depicted. Compared to endosomes in the fusion mixture in which >80% have a membrane potential (left panel), valinomycin collapses the gradient in virtually all the endosomes (right panel). Each panel representative of $n = 6$.

Flow cytometry of the membrane potential on an endosome-by-endosome basis demonstrates the number of endosomes in the fraction in which membrane potential was collapsed (Fig. 4, lower panels). Horizontal axes depict fluorescence of membrane sensitive probe at peak fluorescence 590 ± 10 nm (abscissa) and total fluorescence 585 ± 42 nm (ordinate) with number of endosomes per channel on the vertical axis up out of the page. Each

panel displays the distribution of values from observations on 2000 endosomes. Membrane potential is demonstrable under fusion conditions without valinomycin in >80% of the endosomes (left lower panel), while valinomycin collapses the gradient in virtually all the endosomes (right lower panel). Representative of $n = 4$, $P < 0.05$ valinomycin compared to no valinomycin by Kolgomorov-Smirnoff summation statistics in each case. The use of two measures of fluorescence of the same JC-1 probe at 590 ± 10 nm and 585 ± 42 nm is used to facilitate three dimensional display of the data simply to make changes very apparent visually.

Fusion of Yolk Sac Endosomes

To determine if this distinctive H^+-ATPase dependence of fusion is determined by the highly specialized ''degradative endosomal pathway'' present in select organs, or a property of differentiated mammalian cells lost during the dedifferentiation of cell culture, we examined the H^+-ATPase dependence of fusion in visceral yolk sac cells derived from the Brown Norway rat. This allowed us to test whether fusion was H^+-ATPase dependent in other organ system, the yolk sac, and whether H^+-ATPase dependence of fusion was conserved in a cultured cell system. The BN/MSV immortalized epithelial cells grow well in culture, maintaining some polarized and differentiated features including an abundant brush border and the specialized structures of the ''degradative endosomal pathway'' [20, 22]. Grown in a rotating wall vessel [9], the cells formed almost entirely embryoid bodies consisting of spheres of cells with external brush border, and a fluid filled central cavity. In non-adherent conventional 2-D culture there were 1–2 embryoid bodies/plate, in contrast to >99% embryoid bodies observed after 48 hr cell growth in slow turning lateral vessels. Electron micrographs demonstrate the spherical bodies including maintenance of the specialized endosomal pathway [15, 20, 22, 30] (Fig. 5, upper panels). The embryoid bodies are characterized by an apical microvillar surface (A) and a smooth basolateral surface on the lumen (L) of a fluid filled cavity [left upper panel]. The apical surface has microvilli (slender arrows) and well developed intermicrovillar clefts (bold arrows). Delivery of dyes into the early (fluorescein dextran 10-min exposure) and late (lissamine-rhodamine dextran 10-min exposure 30 min prior to imaging) was imaged by confocal microscopy and demonstrated efficient delivery of dyes into the specialized endosomal pathway (Fig. 5, lower panels). BN/MSV cells demonstrate extraordinarily rapid uptake of fluorescent-dyes compared to many immortal cell lines grown in 2-dimensional culture. Not only does the lower left panel of Fig. 5 demonstrate that green fluorescein-dextran is delivered into many endosomal elements 10 min after presentation, but the fluorescein partially mixes with red rhodamine-dextran delivered 20 min earlier. Hence, dye delivered for fusion studies is throughout the endosomal pathway, as the kinetic definitions of ''early'' and ''late'' endosomal are invalid here.

Having demonstrated that fluorescent-dextran is delivered into the apical endosomal pathway of BN/MSV cells in culture, we were prepared to examine endosomal fusion. Unlike the renal endosomal studies in which the diverse buoyant density of differentiated renal membranes allows facile separation of a highly purified endosomal fraction, the BN/MSV studies rely on the compartmental delivery of fluorescent dextrans. Either fluorescein or rhodamine dextran was entrapped in aliquots of BN/MSV cells in culture, and a crude postnuclear supernatant prepared for fusion studies. During fusion of postnuclear supernatants containing entrapped fluorescein or rhodamine dextran, the fusion was pH gradient independent as collapsing pH gradients with nigericin in the presence of potassium has no effect on fusion (95 ± 4%, $n = 6$). Like endosomes from the renal cortex, fusion of BN/MSV visceral yolk sac endosomes was inhibited by both the v-type H^+-ATPase inhibitor bafilomycin A1 (50 ± 4%, $n = 6$, $P < 0.05$), and collapsing the membrane potential with valinomycin (53 ± 3%, $n = 6$, $P < 0.05$) [Fig. 6].

Discussion

Many common clinical toxins have highly tissue-restricted damage despite systemic administration. Aminoglycosides antibiotics are a classic example in that they are only toxic to the kidney, inner ear and placenta despite intravenous administration, and secondary exposure of all tissues to the drug. Investigation of this tissue-specific toxicity led us to select the kidney and yolk sac placenta as models for our fusion studies.

BN/MSV placental endothelial cells have structural and endosomal kinetic characteristics very different from other cells grown in suspension culture, but very similar to renal proximal tubular cells in vivo [20, 21]. First, the formation of BN cell embryoid bodies, clusters of cells around a fluid filled cavity, ensures marked cell polarity despite suspension culture [15, 21]. The apical surface bears numerous well-developed microvilli, overlying an endosomal pathway characterized by endosomal vesicles, larger endosomal vacuoles, and dense apical tubules [15, 21]. Second, BN cells have a very rapidly active endosomal pathway [21, 22]. This is demonstrated by the substantial uptake of fluorescent dye just 10 min after presentation, and the free intermixing with dye delivered 20 min earlier. The commonality of these structural and functional properties of renal proximal tubular cells and BN/MSV cells, combined with the tissue specific expression of polybasic drug receptors in both cells lines [20, 21, 26], makes them excellent models for studies of the mechanisms of polybasic drug action and toxicity.

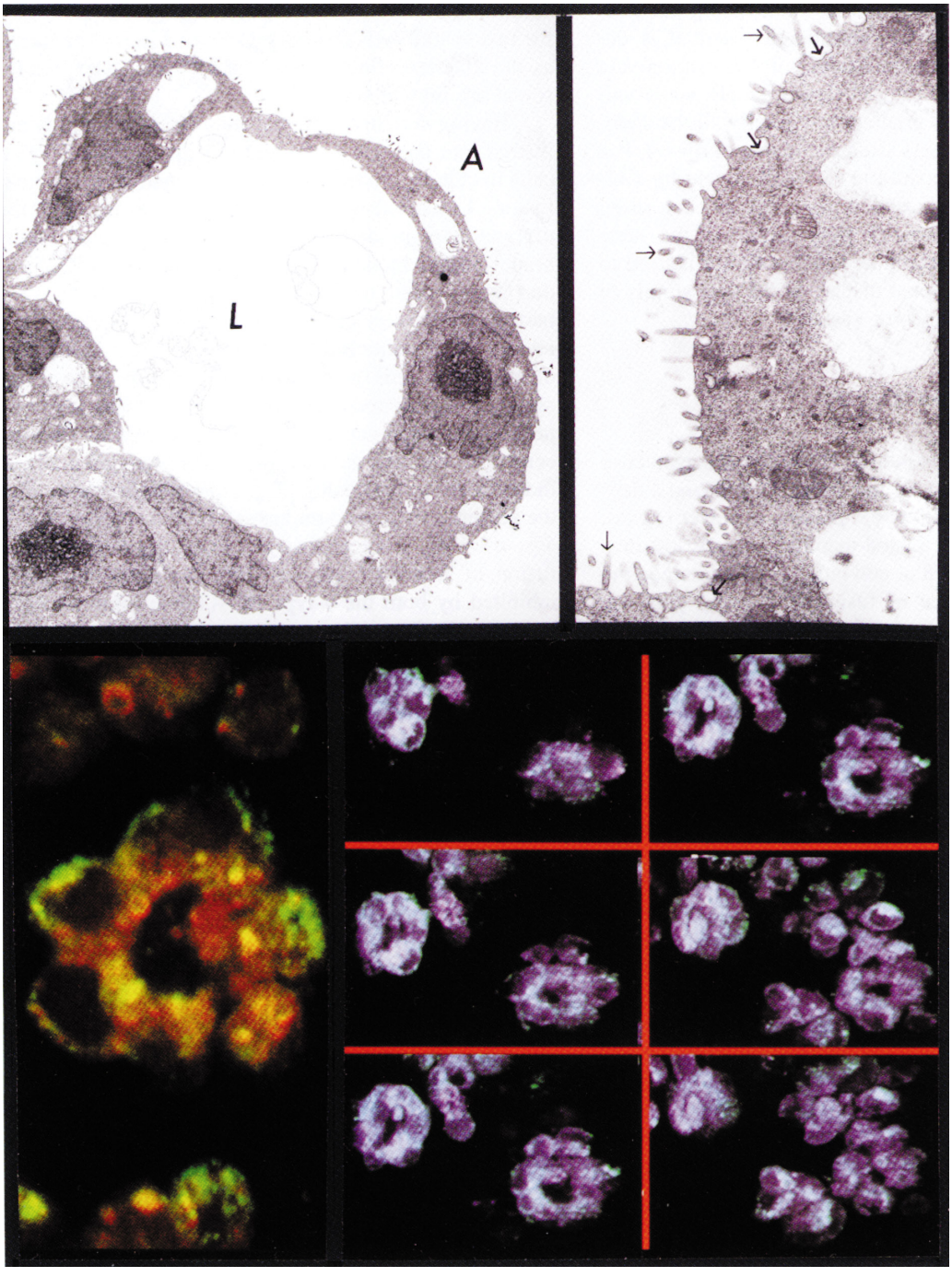

Fig. 5. Structure of visceral yolk sac cell embryoid bodies in culture. (*a*) Electron microscopy. Visceral yolk sac cells form aggregates of interconnecting spheres of cells with central fluid filled cavities (L = lumen) internally, and a well developed brush border apically (A) after culture in slow turning lateral vessels (mag 3,000× upper left panel). The well-defined brush border (slender arrows) and intermicrovillar cleft machinery (bold arrows) of the distinct ''degradative'' endosomal pathway are clearly visible at higher magnification (mag 10,000× upper right panel). (*b*) Confocal microscopy. The distribution and uptake of fluorescein-dextran (in green) [delivered kinetically into an early endosome compartment] and rhodamine-dextran (in red) [delivered kinetically into a late endosome compartment] define the 10 min and 30 min uptake of dyes into different compartments [left lower panel]. The spherical nature and fluid filled core of the embryoid bodies in slow turning lateral vessel culture is emphasized in serial optical sections through a cluster of bodies [lower right panel].

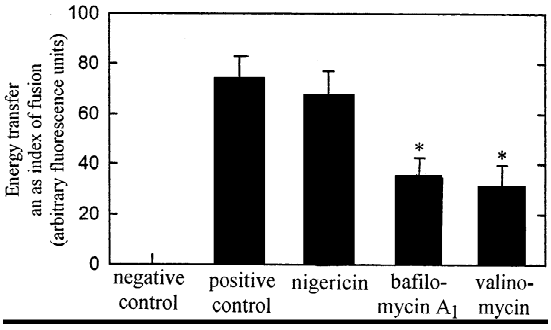

Fig. 6. H^+-ATPase dependence of homotypic rat visceral yolk sac cell early endosome fusion during in vitro reconstitution. Effects of H^+-ATPase agents on cuvette based assay on fusion of rat visceral yolk sac early endosomes using energy transfer from fluorescein to rhodamine to detect fusion. Although the specific H^+-ATPase inhibitor, bafilomycin A1, and collapsing the membrane potential with valinomycin inhibit fusion, collapsing the pH gradient with nigericin has no effect on fusion. Mean ± SE for $n = 8$, *denotes $P < 0.05$ by ANOVA and Scheffe posthoc analysis.

Two principles intended to facilitate tissue-specific identification of the molecular mediators of endosomal fusion guide the design of our studies. First, we use highly purified endosomal populations from differentiated mammalian tissue which contain the channels and receptors of interest [12, 21]. Second, we reconstitute endosomal fusion in vitro [13, 17]. Whereas fusion studies on permeabilized or torn cells in which probes can be delivered intracellularly allow only indirect inferences about mechanisms [1, 6], our in vitro approach of endosomal fusion permits direct dissection of molecular mechanisms [13, 33].

Several lines of evidence suggest that ATPases play a central role in membrane trafficking events including endosomal fusion. First, isolation and cloning of NSF, a cytosolic protein necessary for endosomal fusion, hinged on the finding that it quickly lost its activity in the absence of small quantities of ATP [1]. Second, in BHK cells, the specific v-type H^+-ATPase inhibitor bafilomycin A1 had no effect on membrane internalization or recycling back to the cell surface [4]. However, in the same cell line, inhibition of H^+-ATPase was associated with marked tubule formation in the early endosomal compartment, and endocytosed markers did not enter the late endosomal compartment. Hence, upon inactivation of the proton pump, the formation of vesicular intermediates between early and late endosomes, known as endosomal carrier vesicles, is impaired [4].

Both, the molecular mechanisms responsible for changes in v-type H^+-ATPase activity, and a link between H^+-ATPase and fusion proteins have recently been defined. Disassembly and reassembly of the peripheral subunits (VI sector) from the integral membrane complex (V_o sector) of the v-type H^+-ATPase may be an important regulator of acidification of yeast organelles [18]. Other evidence directly links v-type H^+-ATPases to the fusion complex at the molecular level. Multiple subunits of a H^+-translocating ATPase including the 10 kDa ductin, Ac39 and Ac 116 proteins, co-immunoprecipitate with the synaptobrevin and synaptophysin proteins which form part of biochemical fusion complexes in fresh rat brain [8]. Hence, v-type H^+-ATPase subunits may affect endosomal fusion by direct interactions with the highly conserved synaptobrevin and synaptophysin proteins of the fusion complex [8].

The current study extends observations on the H^+-ATPase dependence of fusion by demonstrating that bafilomycin A1, a highly specific H^+-ATPase inhibitor [28], inhibits homotypic fusion in two different membrane populations derived from endosomes with similar highly specialized features for ''degradative'' endocytosis: endosomes from the renal proximal tubule [12], and early endosomes from visceral yolk sac epithelial cells immortalized in culture [21]. In the latter system, the confocal and electron micrographs demonstrate that BN cells grown in rotating wall vessels form multiple embryoid bodies which provide unequivocal polarity for the apical delivery of fluorescent dextrans added to the buffer [38]. These observations are crucial since, the fusion assay in BN/MSV cell endosomes relies on compartmentation of the fluorescent dextran reporter molecules, the confocal images show distribution of probe in an apical early endosomal compartment utilizing the timing, dosing and delivery of fluorescent dextran used for the fusion assays.

This provides the first direct in vitro evidence that early endosomal fusion is H^+-ATPase dependent. These effects of H^+-ATPase on fusion are mediated by collapse of membrane potential rather than the pH gradient, as the changes are inhibited by collapsing the membrane potential with valinomycin, but not by collapsing pH gradients with nigericin.

The large, slow changes in fluorescence of the new generation of membrane potential sensitive dyes are well suited to demonstrate collapse of membrane potential for fusion experiments [5, 7, 27]. Potentiometric dyes have been used most widely as fast dyes to determine changes in action potentials, bioenergetics, and stimulus-response coupling [5, 7, 27]. Compared to these fast dyes, the new generation of slow response dyes responds in seconds rather than milliseconds, work by bulk redistribution of permeant elements, and demonstrate linearity with much greater changes in fluorescence. While calibration of fluorescence to millivolts remains problematic in many systems [7, 27], we confirm not only the linearity of the relationship between fluorescence and membrane potential, but the generous dynamic range of the new generation of probes facilitates relative if not absolute measurements [7, 27].

A link between membrane potential and membrane

fusion has been observed previously in two other very different biological systems [16, 37]. First, in cultured myoblasts the activation of K(Ca) channels by phloretin dramatically hyperpolarizes the resting membrane potential, and this effect can be reversed upon treatment with tetraethyl ammonium [37]. While phloretin induces precocious membrane fusion, tetraethyl ammonium blocks not only the phloretin-induced precocious fusion but also the spontaneous fusion of the myoblasts. This suggests that the hyperpolarization generated by the reciprocal activation of stretch-activated channels and K(Ca) channels mediates the calcium influx that triggers myoblast fusion [37]. Second, a cytosolic sperm factor triggers calcium oscillations and membrane hyperpolarization in human oocytes [16]. Fertilization of human oocytes by gamete membrane fusion is dependent on hyperpolarization due to this cytosolic sperm protein. Blocking fusion of sperm and oocyte by preventing hyperpolarization is exploited in some new forms of contraception [16]. Taken together with the current observations, these studies suggest membrane potential dependence of membrane fusion may be a more general biological phenomenon.

In the current study, although fusion was membrane potential dependent in both rat renal cortical endosomes and BN/MSV cell endosomes, there were differences in the quantitative dependence of fusion on membrane potential in the two systems. There are two possible reasons for the different degree of membrane potential dependence in the two systems studied. The first reason is the diverse structural and biochemical differences between differentiated rat renal cortical tissue and BN/MSV cells which are immortalized epithelial cells. These two very different systems were chosen for study as they are the only known sources of endosomes from ''degradative'' endosomal pathways which contain the scavenger pathway receptors gp280 and megalin [12, 21, 30]. The second reason is that the renal endosomes are a highly purified fraction [12], while BN cell endosomes fusion relies on compartmentation of the dye [21].

The current observation that fusion of endosomes is dependent on changes in membrane potential provides the first defined mechanism linking functional properties of the final common pathway fusion proteins to the changes in membrane thermodynamics necessary to afford a change in fusion. Changes in membrane thermodynamics require changes in the essential properties of the membranes, which while postulated have never been directly demonstrated [33]. Changes in membrane potential are one mechanism by which changes in fusion properties may be achieved within the rapid restricted time frame of fusion dynamics, which exclude new protein or gene expression [33]. Inhibition of H^+-ATPase prevents formation of both a pH gradient and membrane potential on the treated membranes: the current study provides direct evidence that the membrane potential changes, rather than pH gradients, are the dominant physicochemical transducer of H^+-ATPase dependent fusion properties in renal and BN/MSV cell endosomes.

This research was supported by grants including National Institutes of Health First Award DK46117 (TGH), R21 RR12645 (JHK) and NATO Collaborative Research Grants 94-0750, NASA Grants 9-811 and 8-1362 Basic (TGH; TJG), NASA Graduate Fellowship Award (DLG), NASA UPN 962230132 (TJG), a Veterans's Administration Career Development Award [Research Associate level] (TGH), Fondation Vaincre les Maladie Lysosomales (PJV); and Howard Hughes Medical Institute (confocal microscope of Dr. Sean Carroll). We thank Larry Morrissey for flow cytometry expertise, and Jagriti Chander and Amy M. Amendt-Raduege for excellent technical assistance. Some of the flow cytometry was performed at the Wisconsin Comprehensive Cancer Center. We thank Grayson Scott of the Core Electron Microscopy Facility at the University of Wisconsin—Madison for transmission electron microscopy analysis. We thank Peter I. Lelkes of Sinai Samaritan Medical Center, University of Wisconsin, Milwaukee Clinical Campus for facilitating cultures of BN/MSV cells on one occasion.

References

1. Block, M.R., Glick, B.S., Wilcox, C.A., Wieland, F.T., Rothman, J.E. 1988. Purification of an N-ethylmaleimide-sensitive protein catalyzing vesicle transport. *Proc. Natl. Acad. Sci. USA* **85:**7852–7856
2. Brown, D., Hirsch, S., Gluck, S. 1988. Localization of a proton-pumping ATPase in rat kidney. *J. Clin. Invest.* **82:**2114–2126
3. Chapman, R.E., Munro, S. 1994. Retrieval of TGN proteins from the cell surface requires endosomal acidification. *EMBO J.* **13:**2305–2312
4. Clague, M.J., Urge, S., Aniento, F., Gruenberg, J. 1994. Vacuolar ATPase activity is required for endosomal carrier vesicle formation. *J. Biol. Chem.* **269:**21–24
5. Cornelius, G., Gartner, W., Haynes, D.H. 1974. Cation complexation by valinomycin and nigericin type ionophores registered by the fluorescence signal of T1+. *Biochemistry* **13:**3052–3057
6. Diaz, R., Mayorga, L.S., Colombo, M.I., Lenhard, J.M., Stahl, P.D. 1993. In Vitro studies of endocytic fusion. *Meth. Enzymol.* **221:**201–222
7. Freedman, J.C., Novak, T.S. 1989. Optical measurement of membrane potential in cells, organelles and vesicles. *Meth. in Enzymol.* **172:**102–122
8. Galli, T., McPherson, P.S., De Camilli, P. 1996. The VO sector of the V-ATPase, synaptobrevin, and synaptophysin are associated on synaptic vesicles in a Triton X-100 resistant, freeze-thawing sensitive, complex. complex. *J. Biol. Chem.* **271:**2193–2198
9. Goodwin, T.J., Prewett, T.L., Wolf, D.A., Spaulding, G.F. 1993. Reduced shear stress: A major component in the ability of mammalian tissues to form three-dimensional assemblies in simulated microgravity. *J. Cell. Biochem.* **51:**301–311
10. Hammond, T.G., Majewski, R.R., Kaysen, J.H., Goda, F.O., Navar, G., Pontillon, F., Verroust, P.J. 1997. Gentamicin Inhibits Rat Renal Cortical Homotypic Endosomal Fusion: Role of megalin. *Am. J. Physiol.* **272:**F117–F123
11. Hammond, T.G., Majewski, R.R., Morre, D.J., Schell, K., and Morrissey, L.W. 1993. Forward scatter pulse width signals resolve multiple populations of endosomes. *Cytometry* **14:**411–420
12. Hammond, T.G., Verroust, P. 1994. Heterogeneity of endosomal populations in the rat renal cortex: Light endosomes. *Am. J. Physiol* **266:**C1783–C1794

13. Hammond, T.G., Majewski, R.R., Muse, K.E., Oberley, T.D., Morrissey, L.W., Amendt-Raduege, A.M. 1994. Energy transfer assays of Rat Renal Cortical Endosomal Fusion: Evidence for superfusion. *Am. J. Physiol.* **267:**F1021–F1033
14. Hammond. T.G., Verroust, P.J., Majewski, R.R., Muse, K.E., Oberley, T.D. 1994. Heavy endosomes isolated from the rat renal cortex show attributes of intermicrovillar clefts. *Am. J. Physiol.* **267:**F516–F527
15. Hogan, B.L., Taylor, A., Adamson, E. 1981. Cell interactions modulate embryonal carcinoma cell differentiation into parietal or visceral endoderm. *Nature* **291:**235–237
16. Homa, S.T., Swann, K. 1994. A cytosolic sperm factor triggers calcium oscillations and membrane hyperpolarizations in human oocytes. *Hum. Reprod.* **9:**2356–2361
17. Jo, I., Harris, H.W. Jr., Amendt-Raduege, A.J., Majewski, R.R., Hammond, T.G. 1995. Rat kidney papilla contains abundant synaptobrevin protein that participates in the fusion of anti- diuretic hormone (ADH) water channel-containing endosomes in vitro. *Proc. Natl. Acad. Sci. USA* **92:**1876–1880
18. Kane, P.M. 1995. Disassembly and reassembly of the yeast vacuolar H^+-ATPase in vivo. *J. Biol. Chem.* **270:**17025–17032
19. Kumana, T., Mullock, B.M., Luzio, J.P. 1993. Identification of a protein capable of causing fusion of endosome and lysosome membranes. Biochemical Society Transactions. **21:**299–300
20. Le Panse, S., Galceran, M., Pontillon, F., Lelongt, B., van de Putte, M., Ronco, P., Verroust, P. 1995. Immunofunctional properties of a yolk sac epithelial cell line expressing two proteins of the intermicrovillar areas of proximal tubule cells: inhibition of endocytosis by the specific antibodies. *Eur. J. Cell Biol.* **67:**120–129
21. Le Panse, S., Verroust, P.J., Christensen, E.I. 1997. Internalization and recycling of glycoprotein 280 in BN/MSV yolk sac epithelial cells: A model system of relevance to receptor-mediated endocytosis in the renal proximal tubule. *Exp. Nephrol.* (*in press*)
22. Lloyd, J.B. 1990. Cell physiology of the rat visceral yolk sac: A study of pinocytosis and lysosome function. *Teratology* **41:**383–393
23. Marsh, M., Schmid, S., Kern, H., Harms, E., Male, P. Mellman, I., Helanius, S. 1987. Rapid analytical and preparative isolation of functional endosomes by free flow electrophoresis. *J. Cell Biol.* **104:**875–886
24. Maunsbach, A.B., Christensen, E.I. 1992. Functional ultrastructure of the proximal tubule. *In:* Handbook of Physiology: Renal Physiology, Washington, D.C., Am. Physiol. Soc. 2nd Ed. E.E. Windhager, editor. pp. 41–107. Oxford University Press, New York
25. Mullock, B.M., Perez, J.H., Kuwana, T., Gray, S.R., Luzio, J.P. 1994. Lysosomes can fuse with a late endosomal compartment in a cell-free system from rat liver. *J. Cell Biol.* **126:**1173–1182
26. Moestrup, S.K., Cui, S., Vorum, H., Bregengaard, C., Bjørn, S.E., Norris, K., Gliemann, J., Christensen, E.I. 1995. Evidence that epithelial glycoprotein 330/megalin mediates uptake of polybasic drugs. *J. Clin. Invest.* **96:**1404–1413
27. Montant, V., Farkas, D.L., Loew, L.M. 1989. Dual wavelength ratiometric fluorescence measurements of membrane potential. *Biochemistry* **28:**4536–4539
28. Muroi, M., Shiragami, N., Nagao, K., Yamasaki, M., Takatsuki, A. 1994. Folimycin (concanamycin A) and Bafilomycin A1, Inhibitors specific for V-ATPase exert similar but distinct effects in intracellular translocation and processing of glycoproteins. *Biosci. Biotech. Biochem.* **58:**425–427
29. Murphy, R.F., Roederer, M. 1986. Flow cytometric analysis of endocytic compartment. *In:* Applications of Fluorescence in the Biomedical Sciences, D.J. Morre, editor. pp. 545–563. Alan R. Liss, New York
30. Orlando, R.A., Farquhar, M.G. 1993. Identification of a cell line that expresses a cell surface and a soluble form of the gp330/receptor-associated protein (RAP) Heymann nephritis antigenic complex. *PNAS USA* **90:**4082–4086
31. Paddock, S.W., Langeland, J., DeVries, P., Carroll, S.B. 1993. Three color immunofluorescence imaging of Drosophilia embryos by laser scanning confocal microscopy. *Biotechniques* **14:**42–48
32. Rand, R.P., Kachar, B., Reese, T.S. 1985. Dynamic morphology of calcium-induced interactions between phosphatidylserine vesicles. *Biophys. J.* **47:**483–489
33. Rothman, J.E., Warren, G. 1994. Implications of the SNARE hypothesis for intracellular membrane topology and dynamics. *Current Biology* **4**(3):220–233
34. Sabolic, I., Burckhardt, G. 1990. ATP-driven protein transport in vesicles from the kidney cortex. *Methods in Enzymology* **191:**505–520
35. Saito, A., Pietromonaco, S., Loo, A.K.-C., Farquhar, M.G. 1994. Complete cloning and sequencing of rat gp330/''megalin,'' a distinctive member of the low density lipoprotein receptor gene family. *Proc. Natl. Acad. Sci. USA* **91:**9725–9729
36. Saphon, S., Jackson, J.B., Witt, H.T. 1975. Electrical potential changes, H^+-translocation and phosphorylation induced by short flash excitation in rhodopseudomonas sphaeroides chromatophores. *Biochemica et Biophysica Acta* **408:**67–82
37. Shin, K.S., Park, J.Y., Ha, D.B., Chung, C.H., Kang, M.S. 1996. Involvement of K(Ca) channels and stretch-activated channels in calcium influx, triggering membrane fusion of chick embryonic myoblasts. *Dev Biol* **175:**14–23
38. Uster, P.S. 1993. In situ resonance energy transfer microscopy monitoring membrane fusion in living cells. *Methods in Enzymology* **221:**239–246
39. van Weert, A.W.M., Dunn, K.W., Geuze, H.J., Maxfield, F.R., Stoorvogel, W. 1995. Transport from late endosomes to lysosomes, but not sorting of integral membrane proteins in endosomes, depends on the vacuolar proton pump. *J. Cell Biol.* **130:**821–834
40. Yaver, D.S., Nelson, H., Nelson, N., Klionsky, D.J. 1993. Vacuolar ATPase mutants accumulate precursor proteins in a pre-vacuolar compartment. *J. Biol. Chem.* **268:**10564–10572
41. Young, I.T. 1977. Proof without prejudice: Use of the Kolgomorov-Smirnov test for the analysis of histograms from flow systems and other sources. *J. Histochem. Cytochem.* **25:**935–941